2017 13th. International Computer Engineering Conference (ICENCO)

Learning the Sit-to-Stand Human Behavior: An Inverse Optimal Control Approach

Haitham El-Hussieny[1], Ahmed Asker[2] and Omar Salah[3]

***Abstract*—The issue of understanding the underlying optimality criteria of a certain human movement behavior has received a considerable attention. Recently, an increased interest exists in understanding the Sit-to-Stand (STS) human movement behavior to facilitate the optimal design of assistive systems. Existing research of STS modeling merely depends on some of hard-coded optimality criteria, where the minimum torque change, minimum jerk or/and minimum effort are mainly adopted. In this paper, in the light of the Inverse Optimal Control (IOC) framework, the cost function underlying the STS kinematics is learned from the given human demonstrations. An Inverse Linear Quadratic Regulator (ILQR) algorithm is proposed to find out the unknown cost function that could perfectly reproduce the demonstrated STS data measured with respect to the human greater trochanter (hip) position. The retrieved STS cost function is reasonable and showing an acceptable fit between the simulated trajectories that are generated by the proposed ILQR approach and the given experimental data in terms of the hip position.**

I. Introduction

In recent years, a considerable literature has grown up around the theme of modeling human movement behaviors such as walking, running and grasping, to name a few. Particularly, in Learning by Demonstration (LbD) [1], learning the motion primitives from a set of given human demonstrations could allow artificial agents, such as humanoid robots, to have biologically inspired skills in challenging environments [2]. Moreover, in biomedical research, obtaining a mathematical model of a certain biological movement affords new insights into evaluating the quality of actions for healthy and disordered human subjects [3], [4]. Furthermore, understanding human behaviors could allow the anticipation of human motions beforehand (i.e. intent prediction) which in turns facilitates an intuitive human-guided assistance [5], [6].

Nowadays, the role of incorporating robotic products for performing assistive tasks in the office and home environments, rather than in industries, has been critically highlighted. One example of these products is the assistive devices that can help elderly and disordered people in achieving their prerequisite daily Sit-to-Stand (STS) activities [7], [8], [9], [10]. In fact, the STS human behavior is a complex mobility task, where a high physical effort and a neuromuscular coordination are required to move from sitting to standing [11]. Manual human assistance during STS transfer involves high interaction force and rapid build-up of force which can cause severe neuromuscular injuries to the caregiver [12], [13]. By keeping in mind that, on average, community-dwelling elderly perform around 42 to 49 STS movements per day [14], the requirement for having an assistive robot to support the human STS movement is badly needed. In this context, understanding and modeling of STS movements are required not only for understanding how the nervous system plans the STS motions but also for affording comfort and natural transfer movements by the robotic-based assistive devices.

Fig. 1: A commercial sling used to lift patients from the buttock region. (http://tomoni.co.jp)

Modeling STS transfer based on the dynamic characteristics of the motion requires the identification of many inertial and anatomical parameters which is unsuitable for assistive devices that intended to suit different users. Hence, the kinematic characteristics of the motion have mainly adopted to model the natural STS transfer [15], [16], [7]. Providing assistance at the buttock is one of the most common assisting methods used to reduce the required joint torques during STS transfer. This method is utilized in both manual and robotic-based STS assistance [17]. An example of an assisting sling that is used to facilitate is shown in Figure 1. Therefore, obtaining a model for hip joint motion during STS transfer is an essential step towards providing intuitive robotic-based assistance to the user.

In literature, the cost function underlying the natural STS motion have modeled as a single optimality criterion like the minimum jerk, minimum torque change and minimum effort [15] or a weighted sum of several criteria as presented in [18], [19], [20]. However, a more generalized set of optimality criteria is required to show how each of the kinematic components is contributing to the total cost function of the STS motion. In this paper, the optimality criteria behind the STS movement behavior are retrieved with the help of the IOC framework. The position of the hip joint is measured during the STS motion of healthy human subjects and are identified as optimal or near optimal demonstrations. An Inverse Linear Quadratic Regulator (ILQR) is proposed to retrieve the unknown weighting matrices that best describe and reproduce these given demonstrations.

[1]Electrical Engineering Department, Faculty of Engineering (Shoubra), Benha University, Egypt haitham.elhussieny@feng.bu.edu.eg

[2] Production Engineering and Mechanical Design Department, Mansoura University, Egypt A_askar@mans.edu.eg

[3] Mechanical Engineering Department, Faculty of Engineering, Assiut University, Egypt omar.salah@aun.edu.eg

The rest of this paper is organized as follows, Section II reviews the Linear Quadratic Regulator (LQR) problem. Section III introduces the proposed Inverse LQR (ILQR) approach for modeling the STS human behavior. The application of the proposed ILQR algorithm to the STS behavior is explained alongside the data collection and processing in Section IV. The results are highlighted and discussed in Section V. Finally, Section VI concludes the paper with remarks on the future implications.

II. Review of Linear Quadratic Regulator

The main concern of optimal control theory is to find out the control signals that derive a given system to the desired state while satisfying certain optimality criteria [21]. Linear Quadratic Regulator (LQR) is a variant of optimal control, where the system dynamics are modeled by a set of linear differential equations. In addition, the optimality criteria are described by a quadratic function comprises the system states and inputs. Given a continuous-time linear system,

$$\begin{aligned} \dot{\boldsymbol{x}}(t) &= Ax(t) + Bu(t), \qquad x(0) = x_0 \\ y(t) &= Cx(t) + Du(t), \end{aligned} \tag{1}$$

where A, B, C and D are the system matrices, and $\boldsymbol{x} \in \mathbb{R}^n$, $\boldsymbol{u} \in \mathbb{R}^m$ and $\boldsymbol{y} \in \mathbb{R}^p$ are the state vector, control inputs and the measured outputs respectively. The LQR aims to control the system in (1) such as to minimize the quadratic cost function

$$J = \left\{ \int_0^\infty \left(x(t)^T Q x(t) + u(t)^T R u(t) \right) dt \right\} \tag{2}$$

where $Q \in \mathbb{R}^{n \times n}$ and $R \in \mathbb{R}^{p \times p}$ are the state and input weighting matrices with $Q = Q^T \succeq 0$ and $R = R^T \succ 0$, where $\succeq$ and $\succ$ denote semi-positive definite and positive definite matrices.

Given (A,B) is controllable and (A,C) is detectable, the optimal control input which minimizes the deterministic version of the cost function (2) is given by:

$$u(t) = -Kx(t) \tag{3}$$

where

$$K = R^{-1} B^T P \tag{4}$$

in which P is obtained by solving the following Continuous-time Algebraic Riccati Equation (CARE):

$$A^T P + PA - PBR^{-1}B^T P + Q = 0 \tag{5}$$

In summary, the LQR problem aims to satisfy the quadratic cost function given in (2), given the system dynamics, the set of weighting matrices Q and R.

III. Inverse Linear Quadratic Regulator (ILQR)

In this work, we are interested in solving the inverse problem of the LQR problem mentioned above. Specifically, in the proposed Inverse Linear Quadratic Regulator (ILQR), the objective function defined in (2) is unknown and required, while, on the other hand, the optimal policy in (3) is assumed to be given in a form of some human demonstrated STS motions. Finding the two mentioned weighting matrices Q and R defined in (2), which are unknown in ILQR, could relatively explains the optimality criteria underlying the given STS movement. Definitely, the Q matrix penalizes the deviation of each state from its desired value, while the R penalizes the control efforts $\boldsymbol{u}(t)$ toward minimum values.

Mathematically, while the system matrices in (1) are given, the ILQR problem is formulated as follows, given k measurement samples of a demonstrated behavior $\boldsymbol{y}_h \in \mathbb{R}^{p \times k}$, the goal is to estimate the set of weighting matrices $\hat{Q}$ and $\hat{R}$ that could reproduce the given behavior perfectly. In this paper, the ILQR problem is then formulated as

$$\begin{aligned} \{\hat{Q}, \hat{R}, \hat{\alpha}\} = \min_{Q,R,\alpha} \alpha^2, \quad \text{such that} \\ \|y_h - \hat{y}(Q,R)\|_F^2 \leq \beta, \\ \hat{Q} \succeq 0, \\ \hat{R} \succ 0, \\ \lambda_{max}\left(\begin{bmatrix} \hat{Q} & \mathbf{0} \\ \mathbf{0} & \hat{R} \end{bmatrix} \right) \leq \alpha \\ \lambda_{min}\left(\begin{bmatrix} \hat{Q} & \mathbf{0} \\ \mathbf{0} & \hat{R} \end{bmatrix} \right) \geq 1 \end{aligned} \tag{6}$$

The optimization problem in (6) is formulated, taking the inspiration from [22], in such a way that guarantees regularization for having minimum condition numbers for the retrieved weighting matrices $\hat{Q}$ and $\hat{R}$ which subsequently increases the precision of subsequent arithmetic operations. In other words, minimizing the α value, which is the upper limit for λ_{max} of the block matrix $\begin{bmatrix} \hat{Q} & \mathbf{0} \\ \mathbf{0} & \hat{R} \end{bmatrix}$, alongside the last constraint on λ_{min}, will minimize the condition number of Q and R. This is due to the fact that the condition number of a symmetric matrix can be expressed in terms of its maximum and minimum eigenvalues.

The first constraint in (6) limits the discrepancies between $\boldsymbol{y}_h$, which is the given STS demonstration, and $\hat{\boldsymbol{y}}(Q,R)$, the simulated response for a certain guess of the weighting matrices, where $\| \bullet \|_F$ denotes the Frobenius norm, i.e., $\|A\|_F := \sqrt{trace(A^T A)}$ (for real A). Moreover, the second and third constraints ensure that the estimated $\hat{Q}$ and $\hat{R}$ are in-line with the LQR problem mentioned before. An off-the-shelf Genetic Algorithm (GA) technique [23] is used to solve the optimization problem of the proposed ILQR in (6).

The required matrix $\hat{Q}$ is formed as $\hat{Q} = G + G_u^T$ to obtain a symmetric matrix, where $G = (g_{ij})\ \forall i \geq j$ is an upper triangular matrix with $n(n+1)/2$ elements, while G_u is a matrix formed with the elements of G above the main diagonal. Moreover, the matrix $\hat{R}$ is formulated as a diagonal matrix, i.e. $R = (r_{ij})\ \forall i = j$. All these elements of the weighting

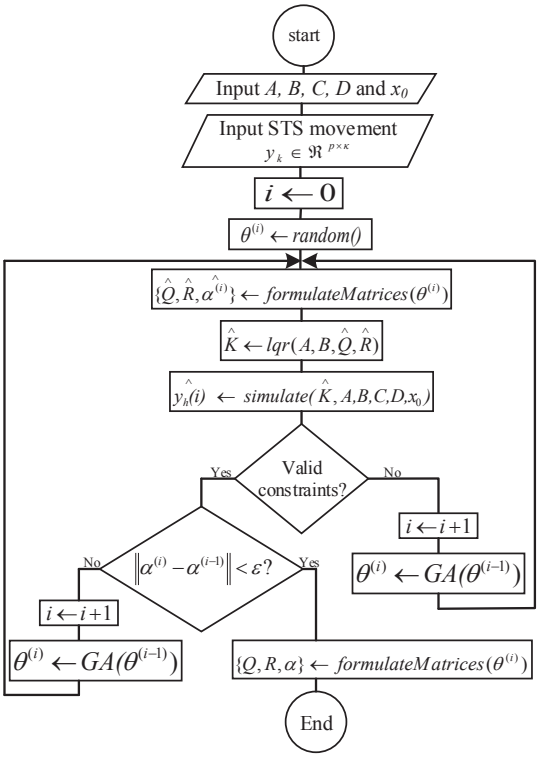

Fig. 2: Flowchart of the proposed ILQR algorithm for retrieving the STS weighting matrices.

matrices besides the candidate α value are appended as a one-dimensional vector $\boldsymbol{\theta}$ which serves as a population for the ILQR optimization problem,

$$\boldsymbol{\theta} := [g_{11}, g_{12}, \ldots g_{nn}, r_1, r_2, \ldots, r_m, \alpha] \tag{7}$$

Figure 2 explains the flowchart of the proposed ILQR procedures to retrieve the Q and R weighting matrices that explain the given STS human behavior. First, the STS behavior model matrices, A, B, C, D, x_0 and the STS measured behavior, $\boldsymbol{y}_h$ are fed to the ILQR algorithm. Then, an initial guess $\boldsymbol{\theta}^{(i)}$ is randomly generated at iteration $i = 0$ to represent the initial GA population. Afterwards, the candidate weighting matrices $\hat{Q}$ and $\hat{R}$ are back formulated from the population vector $\boldsymbol{\theta}^{(i)}$ using the function ***formulateMatrices()*** as shown. Henceforth, the forward LQR problem is solved and the state feedback gain $\hat{K}_i$ is found by solving the CARE mentioned before in (4).Subsequently, the estimated response $\hat{y}$ is obtained by simulating the closed loop system dynamics with $\hat{K}_i$ and the initial condition $\boldsymbol{x}_0$ using the function ***simulate()***. The validity of the constraints in (6) are checked and the algorithm will make another iteration $i+1$ if they are not satisfied. Otherwise, the algorithm will check the convergence over the α value and will repeat again searching for another Q and R weighting matrices in the case of being not converged. On the other hand, if the change in α is less than a certain convergence threshold ϵ, the algorithm will stop and the final candidates of the weighting matrices are formulated and returned as highlighted.

IV. Modeling the Sit-to-Stand Behavior

A. Human Data Collection

Four young and healthy human subjects are being asked to sit on an armless chair with a standard height (45 cm) and stand up to their upright positions naturally. Each participant has performed the STS motion three times with a total of 12 trajectories representing the given demonstrations for the proposed ILQR algorithm. Several markers were attached bilaterally over the required anatomical landmarks (lateral malleolus, femoral condyles, greater trochanter, and acromion) as shown in Figure 3.(a). The 2D positions of the greater trochanter (hip) marker, which is the focus of this research, is captured by the Optitrack (NaturalPoint®) motion capture system with a sampling frequency of 120 Hz. No restrictions regarding the pattern or the speed of the motion are made to make sure that the experiment considers both the user to user and the trial to trail variabilities. The instance of seat-off is assumed to coincide with the time at the peak trunk flexion angle as presented in [24].

B. Formulation of the ILQR for Sit-to-Stand Behavior

Since the proposed ILQR algorithm requires the behavior system matrices defined in (6) as inputs, the kinematic model of the STS movement has been used, where the instantaneous STS state $\vec{X}_t$ at time step t is defined as

$$\vec{X}_t = [x_t \; y_t \; \dot{x}_t \; \dot{y}_t \; \ddot{x}_t \; \ddot{y}_t]^T$$

where the position, velocity, and acceleration of the human hip are measured from the instance of seat-off $\boldsymbol{x}_0$ till the full standing in the upright position as depicted in Figure 4. Velocities and accelerations are found according to difference equations up to a scale factor,

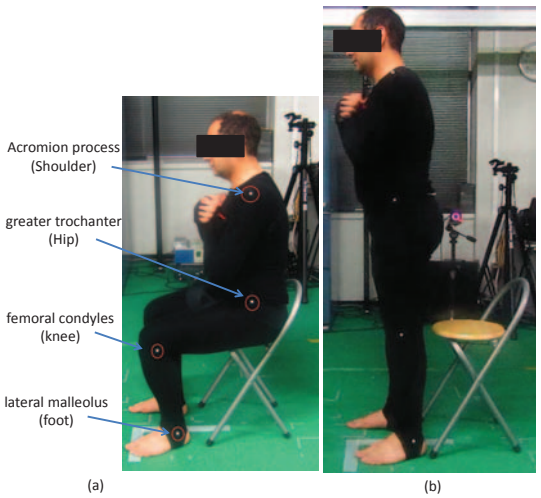

Fig. 3: Configuration of the human subject during the experiment at: (a) the onset of the motion with the anatomical landmarks indicated. (b) motion termination.

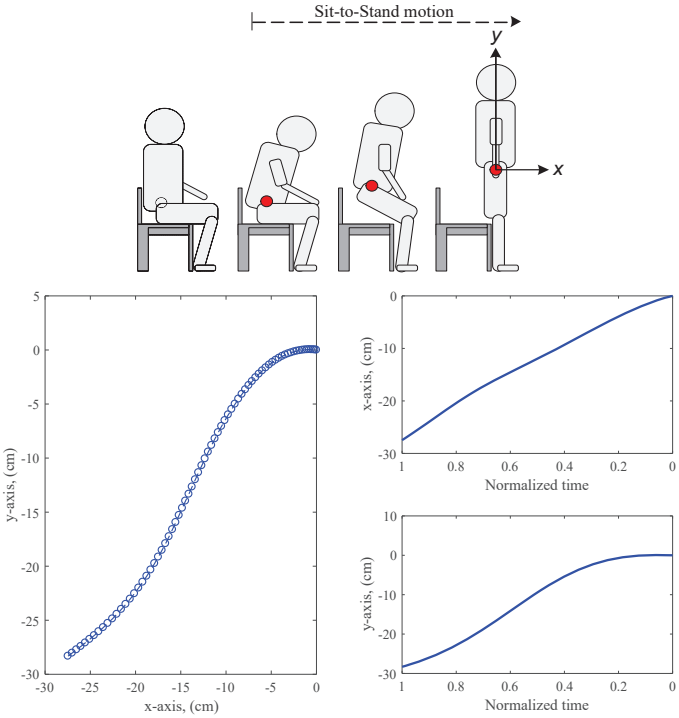

Fig. 4: Illustration of the STS motion with respect to the human hip position highlighted as a red circle. The 2D hip trajectory of one subject demonstration is shown on the left while the horizontal, x, and the vertical, y, motions are shown separately on the right. The time is normalized from one to zero representing the start and the end of the STS motion respectively.

$$\begin{pmatrix} \dot{x}_t \\ \dot{y}_t \end{pmatrix} = \begin{pmatrix} x_t - x_{t-1} \\ y_t - y_{t-1} \end{pmatrix} \tag{8}$$

$$\begin{pmatrix} \ddot{x}_t \\ \ddot{y}_t \end{pmatrix} = \begin{pmatrix} \dot{x}_t - \dot{x}_{t-1} \\ \dot{y}_t - \dot{y}_{t-1} \end{pmatrix} \tag{9}$$

STS movement is expressed as a third-order linear model, where the control input is a vector $\vec{u}_t = [\dddot{x}_t \ \dddot{y}_t]^T$ representing the jerk; the time derivative of the acceleration. We assume the full states of the system are measured to be able to use the LQR problem. Under this dynamic model, the human hip states follow a linear relationship

$$\dot{\vec{X}}_t = A\vec{X}_t + B\vec{u}_t$$

$$\vec{Y}_t = C\vec{X}_t$$

where $A \in \mathbb{R}^{6\times6}$, $B \in \mathbb{R}^{6\times2}$, $C = \mathbf{I}_6$ and $D = \mathbf{0}$ are the dynamics matrices defined as

$$A = \begin{bmatrix} 0 & 0 & 1 & 0 & 0 & 0 \\ 0 & 0 & 0 & 1 & 0 & 0 \\ 0 & 0 & 0 & 0 & 1 & 0 \\ 0 & 0 & 0 & 0 & 0 & 1 \\ 0 & 0 & 0 & 0 & 0 & 0 \\ 0 & 0 & 0 & 0 & 0 & 0 \end{bmatrix} \qquad B = \begin{bmatrix} 0 & 0 \\ 0 & 0 \\ 0 & 0 \\ 0 & 0 \\ 1 & 0 \\ 0 & 1 \end{bmatrix}$$

As noted in Figure 4, the origin of the coordinates for the STS hip motion is located in the final, where the human is in the upright standing position. This makes the starting position for the STS to be negative and increasing to zero at the end. Such kind of projection is consistent with the regulation term of the LQR problem, where the objective is to regulate the system, i.e. derives its states to zero.

V. Results and Discussion

The IQR algorithm is applied to the 12 demonstrated STS behaviors to retrieve the corresponding weighting matrices. Each demonstrated STS is labeled as one scenario and its trajectory is fed to the ILQR algorithm alongside the system matrices mentioned earlier. The pre-defined parameters for the algorithm in (6) are chosen as follows: (i) the discrepancy threshold, $\beta = 50$ and (ii) the threshold of convergence ($\epsilon = 10e^{-4}$).

The main diagonal elements of the Q and R weighting matrices are retrieved separately for the horizontal and the vertical axes for each of the 12 demonstrations. For each axis, the diagonal elements are normalized with respect to their summation to show the percentage of contribution of each kinematic component to the total cost of the STS motion. So, the percentage of the contribution for each of the position, velocity, acceleration and jerk in both horizontal and vertical axes for 12 individuals are plotted in (Figure 5) with their mean, standard deviation, and the 95% confidence intervals. As depicted, for the horizontal x-axis, both the velocity and the acceleration have a large contribution percentage to the total cost function of STS behavior compared to that of either the position or the jerk component. This, in particular, indicates that a higher preference exists for minimizing both the hip velocity and acceleration, around 40% each, during the STS horizontal movement, while around 15% of the cost function is contributed by the minimization of the hip position. This could be explained as during the STS movement, the velocity, and the acceleration are massively penalized in the horizontal direction, which primarily supports the stabilization requirement by penalizing the growing dynamics [25], [26].

However, in the vertical y-axis, the vertical jerk of the hip, $\dddot{y}$, represents the most dominant component with around of 40% percentage of contribution to the STS cost function compared to others. This, in fact, is complying with the well-known minimum-jerk model [27], where to have a smooth biological movement from one point to another, the jerk kinematic component has to be minimum along its trajectory. Hence, regarding the under discussion STS behavior, the vertical motion of the hip during the seat-off is preferred to be smooth with minimum values of the jerk. In the light of these results, the STS behavior, with respect to the human hip, could be identified particularly as a result of two motions. The motion in the horizontal direction, which is responsible for keeping the body center of mass (CoM) within the base of support (foot) while the motion in the vertical direction is responsible for transfer the CoM from it's sitting position to its upright standing position [28]. In other words, The horizontal motion should be achieved in a way to keep balance while the vertical should be done in a way to attain the upright position. Although this results could facilitate a preliminary understanding of the STS behavior, a quantitative clinical

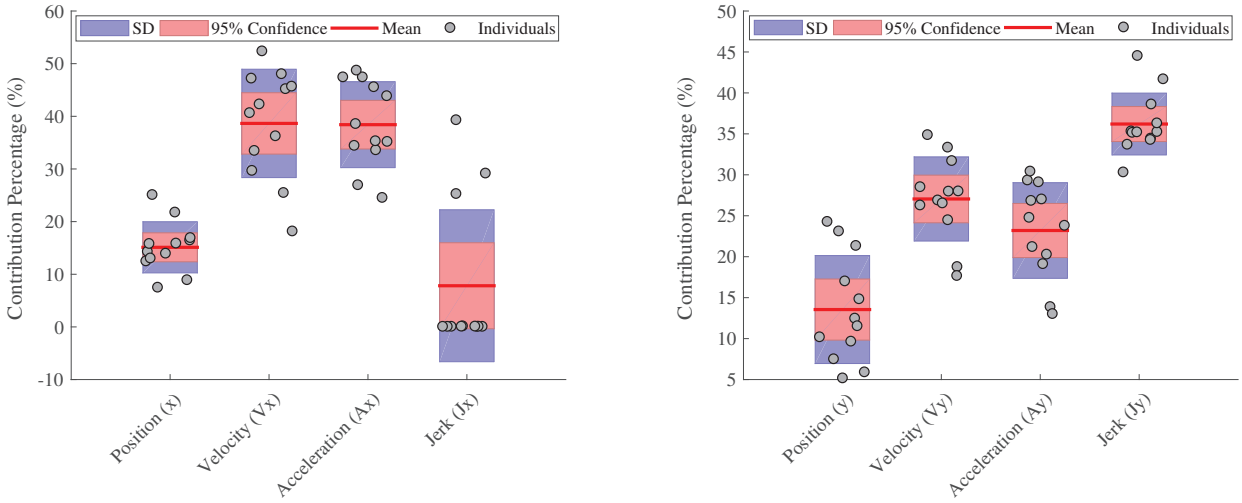

(a) Horizontal Kinematics Components

(b) Vertical Kinematics Components

Fig. 5: The contribution percentage of each of the states and action in the (a) horizontal and (b) vertical axis with respect to the total cost of the STS behavior.

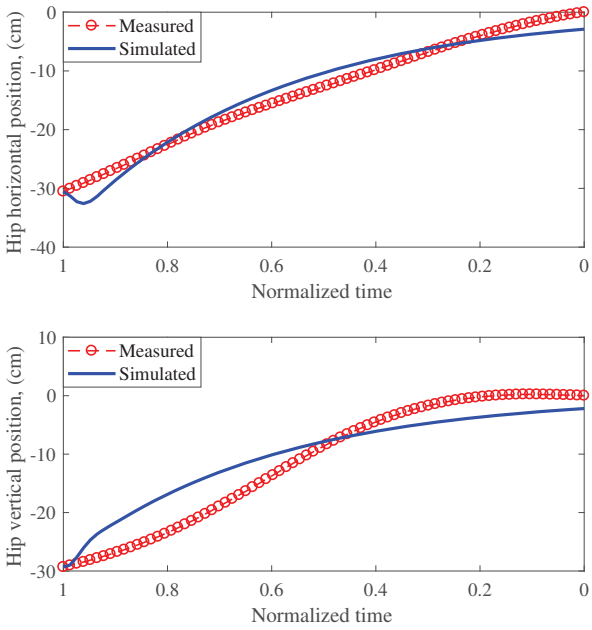

Fig. 6: A Comparison between the measured and the simulated hip position in both horizontal and vertical direction during the STS movement.

study has to be performed to have a much better scientific understanding.

To validate the STS trajectories generated by the proposed ILQR algorithm, the fit of the simulated and the respectively measured hip movement is shown for one arbitrarily chosen STS demonstration in Figure 6. As shown, the simulated model is quite plausible in both the horizontal and the vertical hip position with respect to the measured data. The small discrepancy exists in the resultant fit could perhaps open the door for further future investigations that could be incorporate the dynamics of the STS behavior, such as joint torques, instead of only dealing with the motion kinematics.

VI. Conclusion

A new Inverse Optimal Control (IOC) algorithm called ILQR has been developed for learning the optimization criteria underlying a given Sit-to-Stand (STS) human behavior. The key idea of the proposed algorithm is to retrieve the cost function that could reproduce the given STS behavior perfectly. The developed ILQR has been validated through the application of retrieving the cost function of the STS movements. Although the obtained weighting matrices seem to be reasonable, a further biomedical investigation has to be conducted to confirm the resulting STS model. The obtained supportive results encourage us to further apply the Linear Quadratic Gaussian (LQG) approach in the future to free the mentioned assumption of having full measurable states.

References

[1] B. D. Argall, S. Chernova, M. Veloso, and B. Browning, "A survey of robot learning from demonstration," *Robotics and autonomous systems*, vol. 57, no. 5, pp. 469–483, 2009.

[2] A. Spiers, S. G. Khan, and G. Herrmann, *Human Motion*. Springer International Publishing, 2016, pp. 49–74.

[3] N. Abaid, P. Cappa, E. Palermo, M. Petrarca, and M. Porfiri, "Gait detection in children with and without hemiplegia using single-axis wearable gyroscopes." *PloS one*, vol. 8, no. 9, pp. e73 152–e73 152, 2012.

[4] G. I. Parisi, S. Magg, and S. Wermter, "Human motion assessment in real time using recurrent self-organization," in *2016 25th IEEE International Symposium on Robot and Human Interactive Communication (RO-MAN)*, Aug 2016, pp. 71–76.

[5] O. Salah, A. A. Ramadan, S. Sessa, A. M. F. El-Bab, A. Abo-Ismail, M. Zecca, Y. Kobayashi, A. Takanishi, and M. Fujie, "Sit to stand sensing using wearable imus based on adaptive neuro fuzzy and kalman filter," in *Healthcare Innovation Conference (HIC), 2014 IEEE*. IEEE, 2014, pp. 288–291.

[6] B. I. Ahmad, J. K. Murphy, P. M. Langdon, S. J. Godsill, R. Hardy, and L. Skrypchuk, "Intent inference for hand pointing gesture-based interactions in vehicles," *IEEE transactions on cybernetics*, vol. 46, no. 4, pp. 878–889, 2016.

[7] A. Asker, S. F. M. Assal, M. Ding, J. Takamatsu, T. Ogasawara, and A. M. Mohamed, "Modeling of natural sit-to-stand movement based on minimum jerk criterion for natural-like assistance and rehabilitation," *Advanced Robotics*, vol. 31, no. 17, pp. 901–917, 2017.

[8] A. Asker, S. F. Assal, and A. Mohamed, "Dynamic analysis of a parallel manipulator-based multi-function mobility assistive device for elderly," in *Proc. of IEEE International Conf. on Systems, Man, and Cybernetics (SMC 2015)*, 2015, pp. 1409–1414.

[9] Z. Matjačić, M. Zadravec, and J. Oblak, "Sit-to-stand trainer: an apparatus for training normal-like sit to stand movement," *IEEE Transactions on Neural Systems and Rehabilitation Engineering*, vol. 24, no. 6, pp. 639–649, 2016.

[10] A. Asker, O. Salah, F. El-Bab, M. Ahmed, A. A. Ramadan, S. F. M. Assal, S. Sessa, and A. Abo-Ismail, "Anfis based jacobian for a parallel manipulator mobility assistive device," in *Proc. of UKACC International Conference on Control (CONTROL 2014)*, 2014, pp. 395–400.

[11] P. O. Riley, D. E. Krebs, and R. A. Popat, "Biomechanical analysis of failed sit-to-stand," *IEEE Transactions on rehabilitation engineering*, vol. 5, no. 4, pp. 353–359, 1997.

[12] J. M. Burnfield, Y. Shu, T. W. Buster, A. P. Taylor, M. M. McBride, and M. E. Krause, "Kinematic and electromyographic analyses of normal and device-assisted sit-to-stand transfers," *Gait & posture*, vol. 36, no. 3, pp. 516–522, 2012.

[13] B. McCrory, A. Harlow, and J. M. Burnfield, "Musculoskeletal risk to physical therapists during overground gait training: A case report," in *Proceedings of the Human Factors and Ergonomics Society Annual Meeting*, vol. 58, no. 1. SAGE Publications Sage CA: Los Angeles, CA, 2014, pp. 1219–1223.

[14] R. W. Bohannon, S. R. Barreca, M. E. Shove, C. Lambert, L. M. Masters, and C. S. Sigouin, "Documentation of daily sit-to-stands performed by community-dwelling adults," *Physiotherapy theory and practice*, vol. 24, no. 6, pp. 437–442, 2008.

[15] H. R. Yamasaki, H. Kambara, and Y. Koike, "Dynamic optimization of the sit-to-stand movement," *Journal of applied biomechanics*, vol. 27, no. 4, pp. 306–313, 2011.

[16] O. Salah, A. A. Ramadan, S. Sessa, A. A. Ismail, M. Fujie, and A. Takanishi, "Anfis-based sensor fusion system of sit-to-stand for elderly people assistive device protocols," *International Journal of Automation and Computing*, vol. 10, no. 5, pp. 405–413, 2013.

[17] R. Kamnik and T. Bajd, "Standing-up robot: an assistive rehabilitative device for training and assessment," *Journal of medical engineering & technology*, vol. 28, no. 2, pp. 74–80, 2004.

[18] J. Kuželički, M. Žefran, H. Burger, and T. Bajd, "Synthesis of standing-up trajectories using dynamic optimization," *Gait & posture*, vol. 21, no. 1, pp. 1–11, 2005.

[19] M. Geravand, P. Z. Korondi, C. Werner, K. Hauer, and A. Peer, "Human sit-to-stand transfer modeling towards intuitive and biologically-inspired robot assistance," *Autonomous Robots*, vol. 41, no. 3, pp. 575–592, 2017.

[20] M. Sadeghi, M. E. Andani, M. Parnianpour, and A. Fattah, "A bio-inspired modular hierarchical structure to plan the sit-to-stand transfer under varying environmental conditions," *Neurocomputing*, vol. 118, pp. 311–321, 2013.

[21] D. E. Kirk, *Optimal control theory: an introduction*. Courier Corporation, 2012.

[22] M. C. Priess, R. Conway, J. Choi, J. M. Popovich, and C. Radcliffe, "Solutions to the inverse lqr problem with application to biological systems analysis," *IEEE Transactions on Control Systems Technology*, vol. 23, no. 2, pp. 770–777, 2015.

[23] K. Deb, A. Pratap, S. Agarwal, and T. Meyarivan, "A fast and elitist multiobjective genetic algorithm: Nsga-ii," *IEEE transactions on evolutionary computation*, vol. 6, no. 2, pp. 182–197, 2002.

[24] K. Tanghe, A. Harutyunyan, E. Aertbeliën, F. De Groote, J. De Schutter, P. Vrancx, and A. Nowé, "Predicting seat-off and detecting start-of-assistance events for assisting sit-to-stand with an exoskeleton," *IEEE Robotics and Automation Letters*, vol. 1, no. 2, pp. 792–799, 2016.

[25] K. Mombaur, A. Truong, and J.-P. Laumond, "From human to humanoid locomotionan inverse optimal control approach," *Autonomous robots*, vol. 28, no. 3, pp. 369–383, 2010.

[26] H. El-Hussieny, A. Abouelsoud, S. F. Assal, and S. M. Megahed, "Adaptive learning of human motor behaviors: An evolving inverse optimal control approach," *Engineering Applications of Artificial Intelligence*, vol. 50, pp. 115–124, 2016.

[27] T. Flash and N. Hogan, "The coordination of arm movements: an experimentally confirmed mathematical model," *Journal of neuroscience*, vol. 5, no. 7, pp. 1688–1703, 1985.

[28] C. J. Winstein, D. K. Rose, S. M. Tan, R. Lewthwaite, H. C. Chui, and S. P. Azen, "A randomized controlled comparison of upper-extremity rehabilitation strategies in acute stroke: a pilot study of immediate and long-term outcomes," *Archives of physical medicine and rehabilitation*, vol. 85, no. 4, pp. 620–628, 2004.